

Support Information

Dopant effect on the optical and thermal properties of 2D organic-Inorganic Hybrid Perovskite (HDA)₂PbBr₄

Zhi Lin^{[a], #}, *Ya-Nan Wu*^{[a], #}, *Si-Yu Xu*^[a], *Bi-Cui Chen*^[a], *Pei-Wen Huang*^[a], *Xing-Hui Qi*

[b]*, *Yang-Peng Lin*^[a*], *Ke-Zhao Du*^[a*]

[a] College of Chemistry and Materials Science, Fujian Provincial Key Laboratory of Advanced Materials Oriented Chemical Engineering, Fujian Normal University, Fuzhou, 350007, China

[b] Joint School of National University of Singapore and Tianjin University, International Campus of Tianjin University, Fuzhou 350207, China

**Correspondent Emails:*

duke@fjnu.edu.cn (K.-Z. D.)

xhqi@tjufz.org.cn (X. Q.),

lyp.fjnu@outlook.com

These authors contribute equally to this work.

Experimental Section:

Materials: lead (II) bromide (PbBr_2 , 99%, Adamas), hydrobromic acid (HBr , 48%w/w, Aladdin), methanol (CH_3OH , $\geq 99.5\%$, Aladdin), ethyl acetate ($\text{C}_4\text{H}_8\text{O}_2$, 99.50%, Shanghai Shenbo Chemical), anhydrous diethyl ether($(\text{C}_2\text{H}_5)_2\text{O}$, AR, Greagent), dopamine hydrochloride ($\text{C}_8\text{H}_{11}\text{NO}_2\cdot\text{HCl}$, 98%, Aladdin), manganese (II) oxide (MnO , 99.5% Macklin), antimony (III) oxide (Sb_2O_3 , 99%, Adamas), bismuth (III) oxide (Bi_2O_3 , 99%, Adamas),

Preparation of $(\text{HDA})_2\text{PbBr}_4$ Stoichiometric amounts of PbBr_2 (22.0 mg, 0.06 mmol) and $\text{C}_8\text{H}_{11}\text{NO}_2\cdot\text{HCl}$ (22.8 mg, 0.12 mmol) were dissolved in concentrated hydrobromic acid (0.5 mL). Then, 1 mL CH_3OH was slowly added on the top of the mixed solution along the wall of bottle. After 3 days, we can obtain the colorless flakes crystals in the bottom of the bottle. The yield of $(\text{HDA})_2\text{PbBr}_4$ single crystal is 25% - 35% (based on Pb).

Preparation of Mn-1 single crystal. Stoichiometric amounts of PbBr_2 (110.1 mg, 0.3 mmol), $\text{C}_8\text{H}_{11}\text{NO}_2\cdot\text{HCl}$ (113.8 mg, 0.6 mmol) and MnO (120.6 mg, 1.7 mmol) were dissolved in concentrated hydrobromic acid (2.5 mL). Then, 2.5 mL $(\text{C}_2\text{H}_5)_2\text{O}$ was slowly added on the top of the mixed solution along the wall of bottle. After 3-5 days, kept at room temperature, we can obtain the colorless gray flake crystals in the bottom of the bottle. Mn^{2+} doped $(\text{HDA})_2\text{PbBr}_4$ samples with different doping concentration were synthesized by increasing MnO with corresponding stoichiometric ratio.

Preparation of Sb-1 single crystal. Stoichiometric amounts of PbBr_2 (110.1 mg, 0.3 mmol), $\text{C}_8\text{H}_{11}\text{NO}_2\cdot\text{HCl}$ (113.8 mg, 0.6 mmol) and Sb_2O_3 (145.8 mg, 0.5 mmol) were dissolved in concentrated hydrobromic acid (2.5 mL). Then, 2.5 mL $\text{C}_4\text{H}_8\text{O}_2$ was slowly added on the top of the mixed solution along the wall of bottle. After 3-5 days, kept at room temperature, we can obtain the yellow flake transparent crystals in the bottom of the bottle. Sb^{3+} doped $(\text{HDA})_2\text{PbBr}_4$ samples with different doping concentration were synthesized by increasing Sb_2O_3 with corresponding stoichiometric ratio.

Preparation of Bi-1 single crystal. Stoichiometric amounts of PbBr_2 (88.0 mg, 0.24 mmol), $\text{C}_8\text{H}_{11}\text{NO}_2\cdot\text{HCl}$ (91.0 mg, 0.48 mmol) and Bi_2O_3 (93.2 mg, 0.2 mmol) were dissolved in concentrated hydrobromic acid (2 mL). Then, 2 mL $\text{C}_4\text{H}_8\text{O}_2$ was slowly added on the top of the mixed solution along the wall of bottle. After 3-5 days, kept

at room temperature, we can obtain the deep brown crystals in the bottom of the bottle. Bi³⁺ doped (HDA)₂PbBr₄ samples with different doping concentration were synthesized by increasing Bi₂O₃ with corresponding stoichiometric ratio.

Powder X-ray diffraction (PXRD) measurements. The PXRD data was obtained using Rigaku Miniflex diffractometer (Cu K α , $\lambda = 1.5418 \text{ \AA}$) at room temperature in the range of $2\theta = 5 - 65^\circ$. The simulated PXRD pattern was calculated by Mercury software according to the corresponding CIF file of single crystal.

ICP-OES. American Agilent ICP-OES 730.

X-ray photoelectron spectroscopy (XPS) measurements. XPS spectra were analyzed by Thermo ESCALAB 250Xi.

EDS. EDS was obtained by a JSM - 7500F, JEOL scanning electron microscope (SEM).

UV/Vis Spectra. The UV/vis spectra were recorded within the 800 – 200 nm range using an UV-2600 spectrometer from Shimadzu at room temperature.

TGA. TG analysis was proceeded on a NETZSCH STA 449F3 instrument at a heating rate of 10 K min^{-1} under a dry N₂ atmosphere from 20 to 1000 °C.

DSC. DSC analysis was proceeded on a TA - Q20 of American instrument. The DSC of 1 and PDA-1 was conducted from 30 to 230 °C under a nitrogen atmosphere at a heating/cooling rate of 5 K min^{-1} .

Photoluminescence. Room time PL and PLE were recorded on PerkinElmer LS55 fluorescence spectrometer.

PL decay spectra. FLS1000 Photoluminescence Spectrometer, Edinburgh Instruments Ltd. Variation Photoluminescence spectrometer was measured at FLS1000 Photoluminescence Spectrometer (Edinburgh Instruments Ltd) equipped with a liquid-nitrogen cooled photomultiplier tube as a detector (Hamamatsu, R5509, InP/InGaAsP).

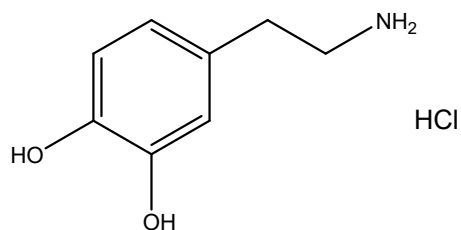


Figure S1. Structural formula of protonated dopamine.

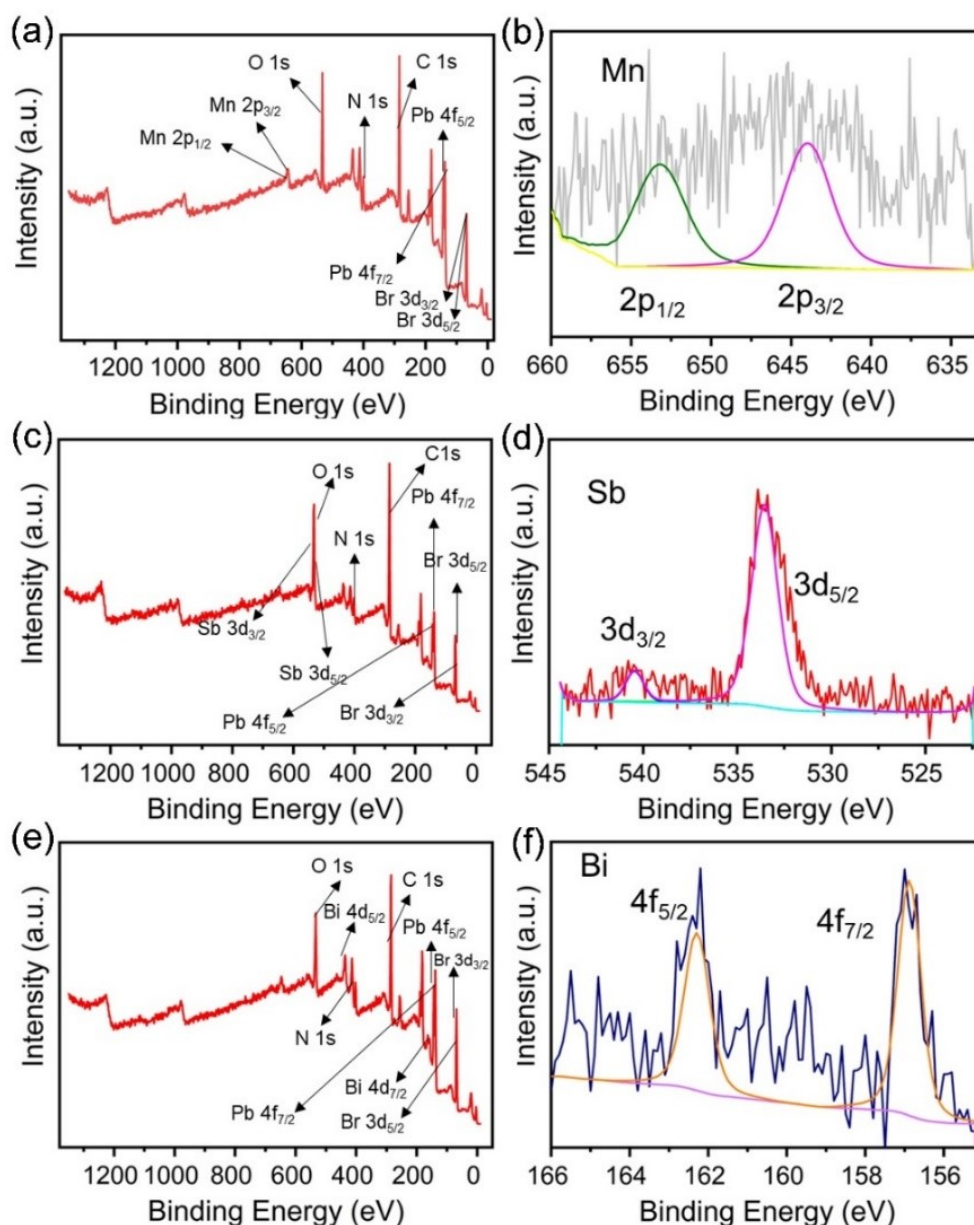


Figure S2. (a) The XPS spectrum of Mn-1 survey scan; (b) Fine spectrum of 2p orbital of Mn in crystal Mn-1; (c) The XPS spectrum of Sb-1 survey scan; (d) Fine spectrum of 3d orbital of Sb in crystal Sb-1; (e) The XPS spectrum of Bi-1 survey scan; (f) Fine spectrum of 4f orbital of Bi in Bi-1 crystal.

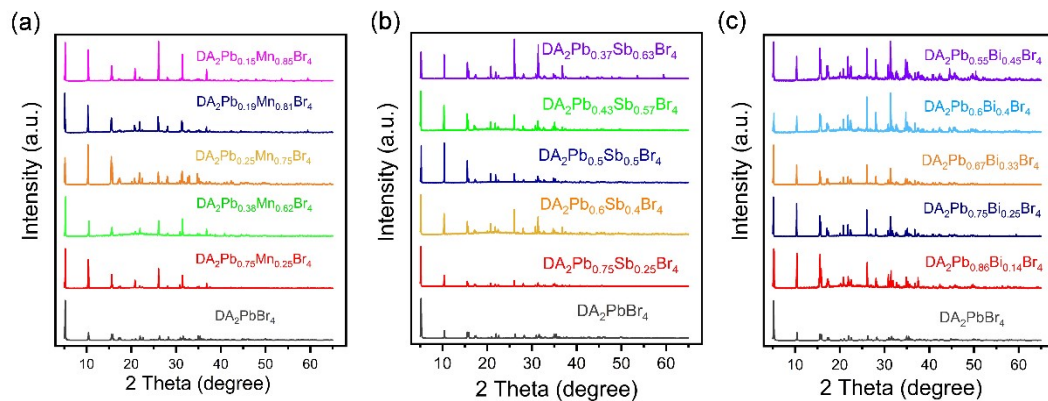


Figure S3. (a) PXRD patterns of crystal **1** doped Mn^{2+} with different Mn concentrations; (b) PXRD patterns of crystal **Sb-1** with different Sb concentrations; (c) PXRD patterns of crystal **Bi-1** with different Bi concentrations.

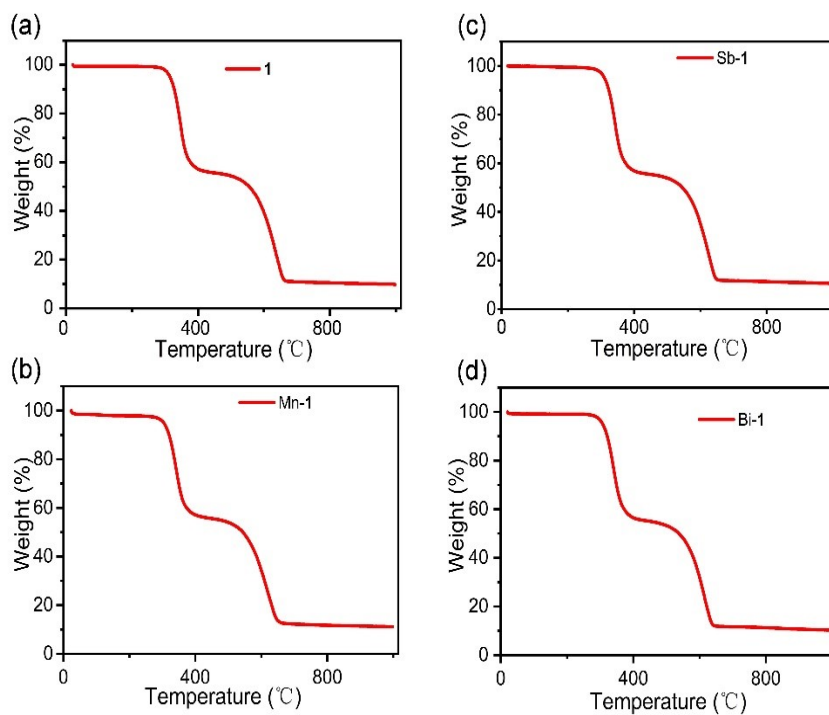


Figure S4. (a)-(d) Thermogravimetric curve of crystal **1**, **Mn-1**, **Sb-1**, **Bi-1**.



Figure S5. Photos of crystal **1**

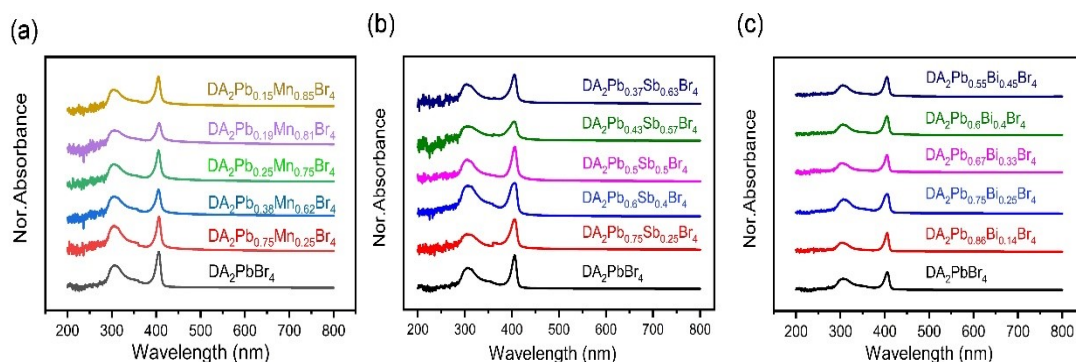


Figure S6. (a) Ultraviolet absorption spectra of crystal **1** doped Mn^{2+} at different concentrations; (b) Ultraviolet absorption spectra of crystal **1** doped Sb^{3+} at different concentrations; (c) Ultraviolet absorption spectra of crystal **1** doped Bi^{3+} at different concentrations. The atomic ratio in the formula represents the feeding ratio.

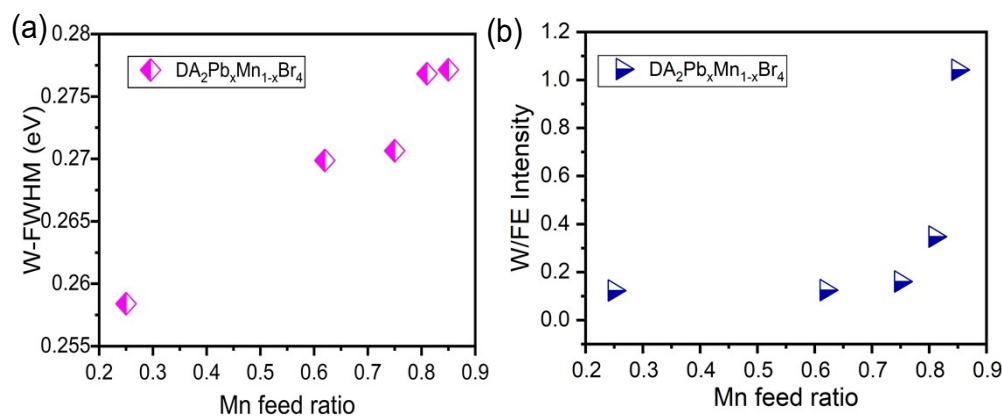


Figure S7. Variation trend of FWHM of peak W with the increase of Mn doping concentration; (b) The ratio of fluorescence intensity of peak W to the peak FE with the increase of Mn doping concentration.

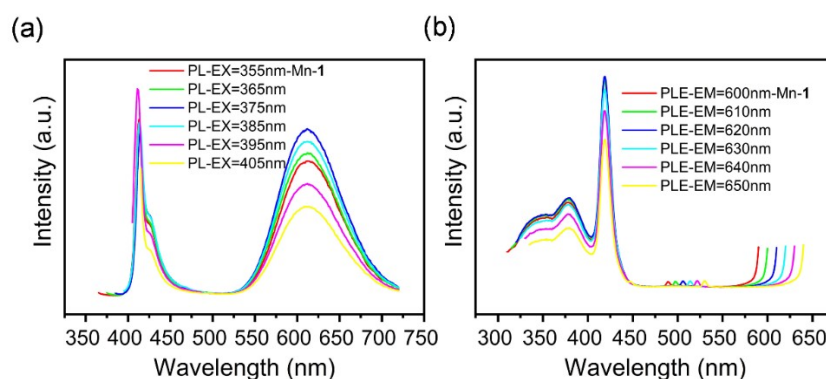


Figure S8. (a) Wavelength-dependent PL spectra of Mn-1 at room temperature; (b)

Wavelength-dependent PLE spectra of Mn-1 at room temperature.

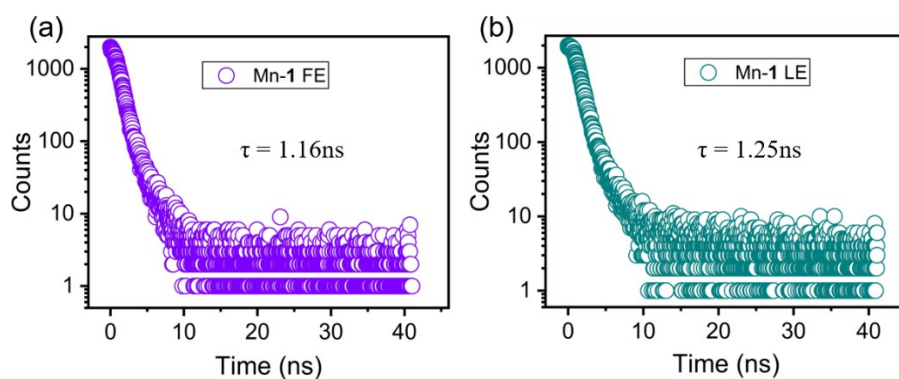


Figure S9. PL lifetime of peak FE of crystal Mn-1 at room temperature; (b) PL lifetime of peak LE of crystal Mn-1 at room temperature.

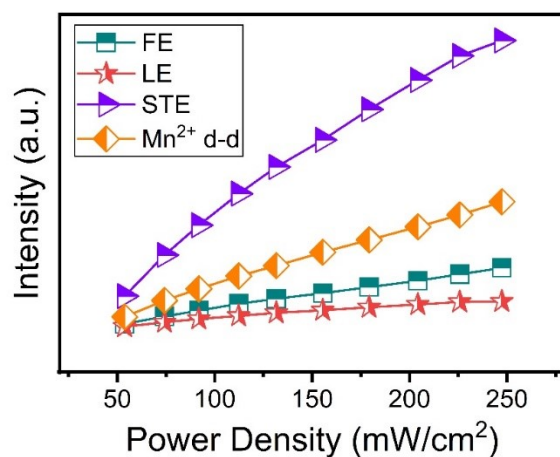


Figure S10. Powder density-dependent PL intensity of peak FE, LE, STE and Mn^{2+} d-d in Mn-1 at 80K.

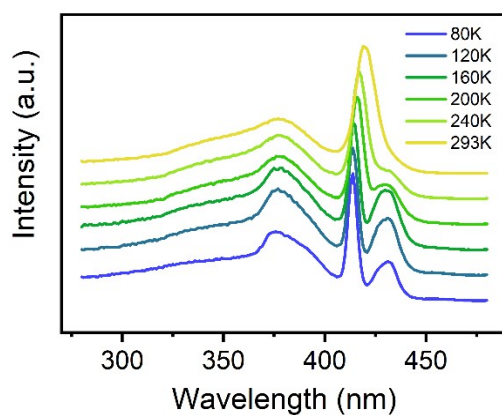


Figure S11. Temperature-dependent PLE spectra of Mn-1.

The emission wavelength is 650 nm.

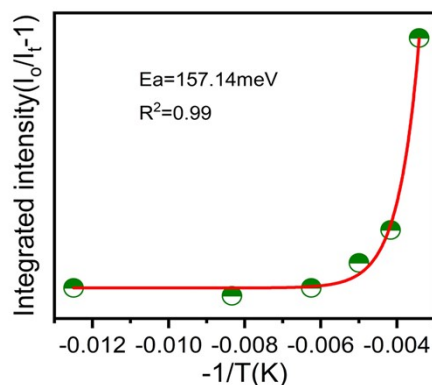


Figure S12 Temperature dependent integrated intensity of 430 nm peak in the PLE of Mn-1 sample. The data is fitted by Arrhenius formula.

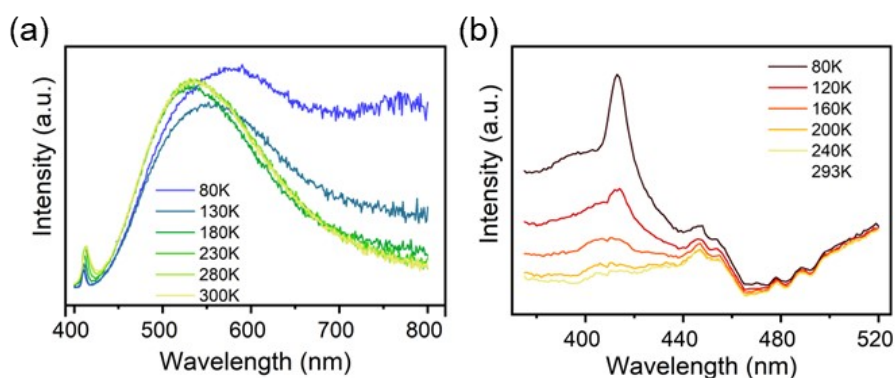


Figure S13. (a) Temperature-dependent PL spectra of Sb-1. The excitation wavelength is 375 nm (b) Temperature-dependent PLE spectra of Sb-1. The emission wavelength is 750 nm.

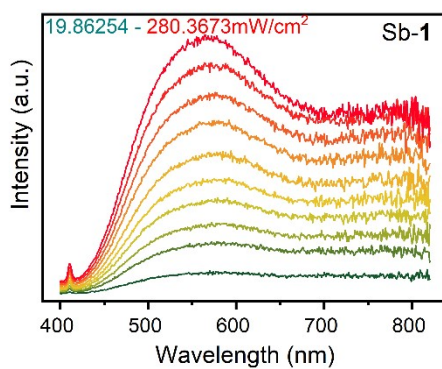


Figure S14. Powder density-dependent PL spectra of Sb-1 at 80K. The excitation wavelength is 375 nm.

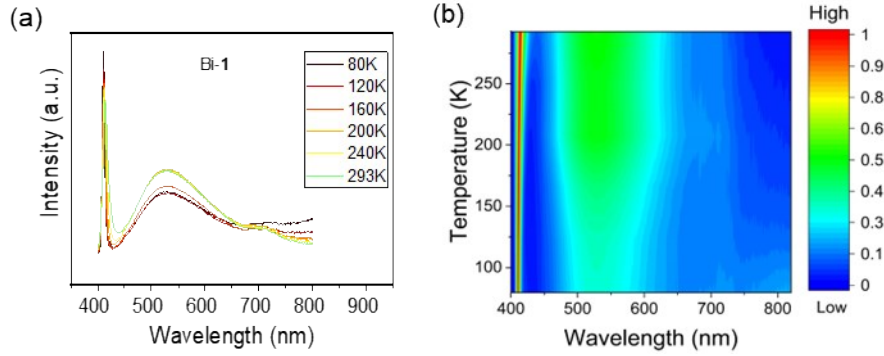


Figure S15. (a) Temperature-dependent PL spectra of Bi-1. The excitation wavelength is 365 nm. (b) Pseudo-color PL image of Bi-1 under different temperatures.

Table S1. ICP-OES data of doping with different doping concentrations of Mn^{2+} and maximum doping concentration of Sb^{3+} and Bi^{3+} .

Mn-to-Pb molar feed ratio (nominal)	Actual concentration%	Pb^{2+} Actual concentration%	Mn^{2+} actual Mn^{2+} -to- Pb^{2+} molar ratio
$DA_2Pb_{0.75}Mn_{0.15}Br_4$	0.1234%	0.00019%	0.00154%
$DA_2Pb_{0.38}Mn_{0.62}Br_4$	0.1192%	0.0014%	0.0117%
$DA_2Pb_{0.25}Mn_{0.75}Br_4$	0.1226%	0.00178%	0.01451%
$DA_2Pb_{0.19}Mn_{0.81}Br_4$	0.1222%	0.0027%	0.0027%
$DA_2Pb_{0.15}Mn_{0.85}Br_4$	0.123%	0.0063%	0.051%

Sb-to-Pb molar feed ratio (nominal)	Actual concentration%	Pb^{2+} Actual concentration%	Sb^{3+} Actual Sb^{3+} -to- Pb^{2+} molar ratio
$DA_2Pb_{0.37}Sb_{0.63}Br_4$	0.121%	0.00220%	0.0181%

Bi-to-Pb molar feed ratio (nominal)	Actual concentration%	Pb^{2+} Actual concentration%	Bi^{3+} Actual Bi^{3+} -to- Pb^{2+} molar ratio
$DA_2Pb_{0.55}Bi_{0.45}Br_4$	0.1174%	0.0013%	0.011%

Table S2. EDS data sheet with different ions doped.

	Element	Weight %	Atomic %
Mn-1	Br L	26.78	7.19
	Pb M	14.19	1.47
	Mn K	0.31	0.12
Sb-1	Br L	29.92	8.31
	Pb M	14.92	1.60
	Sb L	0.12	0.02
Bi-1	Br L	26.94	7.25
	Pb M	13.48	1.40
	Bi M	1.80	6.71

Table S3. Room-temperature PL data of Mn²⁺ doped. W/FE represents the intensity ratio of the peak W to the peak FE.

	Peak W FWHM (eV)	Peak W (Intensity)	Peak FE (Intensity)	W/FE
DA ₂ Pb _{0.75} Mn _{0.25} Br ₄	0.25841	2.26923E6	1.8451E7	0.1230
DA ₂ Pb _{0.38} Mn _{0.62} Br ₄	0.26988	1.24457E6	1.0007E7	0.1244
DA ₂ Pb _{0.25} Mn _{0.75} Br ₄	0.27065	2.86525E6	1.7817E7	0.1608
DA ₂ Pb _{0.19} Mn _{0.81} Br ₄	0.27683	1.67419E6	4.8241E6	0.3407
DA ₂ Pb _{0.15} Mn _{0.85} Br ₄	0.27714	7.41017E6	7.1064E6	1.0427

Table S4. Power-dependent FWHM data of peak FE and LE in Mn-1 at 80K.

Mn-1-80K-Power Density (mW/c m ²)	FE-integrated intensity	LE- integrated intensity	FE-area percentage	LE-area percentage
---	----------------------------	--------------------------------	-----------------------	-----------------------

19.86254	13470.37491	16159.36554	45.46235	54.53765
47.36451	31165.94907	36891.19278	45.7938	54.2062
71.04677	44630.03085	50662.57657	46.83473	53.16527
98.54874	61159.57342	63545.23277	49.04348	50.95652
124.5228	71415.36428	79848.98831	47.21229	52.78771
156.6085	87128.24302	87727.26698	49.82871	50.17129
188.6941	102981.3988	97986.40625	51.24273	48.75727
222.3076	121403.8529	109503.1142	52.57696	47.42304
251.3375	134660.0381	127828.214	51.30136	48.69864
280.3673	152119.4103	130441.5095	53.83597	46.16403

Table S5. Temperature-dependent peak position and FWHM of peak FE and LE in Mn-1.

	Peak Position-FE	FWHM-FE	Peak Position-LE	FWHM-LE
80K	3.02002	0.01886	2.99673	0.05936
120K	3.01792	0.02083	2.99778	0.05877
160K	3.01381	0.02581	2.98948	0.06866
200K	3.00898	0.03193	2.97466	0.08596
240K	3.00426	0.03878	2.95487	0.10069
293K	2.99672	0.0486	2.92368	0.13906

Table S6. Temperature-dependent FWHM of exciton peak in the PL spectra of Sb-1.

	FWHM	Peak Position (eV)
80K	0.03299	3.01816
120K	0.03631	3.01637
160K	0.04273	3.01299

200K	0.04746	3.00831
240K	0.05879	3.00085
293K	0.06072	2.99794

Table S7. Temperature-dependent FWHM of exciton peak in the PL spectra of Bi-1.

	FWHM (eV)	Peak Position (eV)
80K	0.04524	3.02067
120K	0.04879	3.01926
160K	0.05369	3.01611
200K	0.06108	3.01134
240K	0.06533	3.00489
293K	0.07649	2.99618